대 한 조 선 학 회 논 문 집
제 47 권 제 3 호 2010 년 6 월

Journal of the Society of Naval Architects of Korea
Vol. 47, No. 3, pp. 291-305, June 2010
DOI: 10.3744/SNAK.2010.47.3.291

3 차원 시간영역 근사비선형 2 차경계요소법에 의한 선체의 대진폭 운동 및 파랑하중 계산

홍도천*, 홍사영†**, 성홍근**

충남대학교 첨단수송체연구소*
한국해양연구원 해양시스템안전연구소**

Estimation of Large Amplitude Motions and Wave Loads of a Ship Advancing in Transient Waves by Using a Three Dimensional Time-domain Approximate Body-exact Nonlinear 2nd-order BEM

Do-Chun Hong*, Sa-Young Hong†** and Hong-Gun Sung**

Center for Advanced Transportation Vehicles, Chungnam National University*
Maritime and Ocean Engineering Research Institute, KORDI**

Abstract

A three-dimensional time-domain calculation method is of crucial importance in prediction of the motions and wave loads of a ship advancing in a severe irregular sea. The exact solution of the free surface wave-ship interaction problem is very complicated because of the essentially nonlinear boundary conditions. In this paper, an approximate body nonlinear approach based on the three-dimensional time-domain forward-speed free-surface Green function has been presented. The Froude-Krylov force and the hydrostatic restoring force are calculated over the instantaneous wetted surface of the ship while the forces due to the radiation and scattering potentials over the mean wetted surface. The time-domain radiation and scattering potentials have been obtained from a time invariant kernel of integral equations for the potentials which are discretized according to the second-order boundary element method (Hong and Hong 2008).

접수일: 2009 년 12 월 3 일, 승인일: 2010 년 3 월 22 일
†교신저자: sayhong@moeri.re.kr 042-866-3930

The diffraction impulse-response functions of the Wigley seakeeping model advancing in transient head waves at various Froude numbers have been presented. A simulation of coupled heave-pitch motion of a long rectangular barge advancing in regular head waves of large amplitude has been carried out. Comparisons between the linear and the approximate body nonlinear numerical results of motions and wave loads of the barge at a nonzero Froude number have been made.

※Keywords: Time-Domain Approximate Body Nonlinear Ship Motion and Wave Loads (시간영역 근사비선형 선체운동 및 파랑하중), Forward-Speed Diffraction Impulse-Response Function (전진속도 충격응답함수), Three-Dimensional Time-Domain Forward-Speed Free-Surface Green Function (3DTFFG: 3 차원 시간영역 전진속도 자유표면 그린함수), Time-Domain Green Integral Equation (시간영역 Green 적분방정식), Forward-Speed Radiation Memory Function (전진속도 운동이력함수), 2nd Order Boundary Element Method (2 차경계요소법)

1. INTRODUCTION

The three-dimensional time-domain free-surface Green function under integral form, associated with a point source in arbitrary motion has been presented by Stoker (1957). Liapis and Beck (1985) have presented the Green integral equation (also referred to as source and normal doublet distribution method) for the radiation problem of a ship advancing with a constant forward speed using a three-dimensional time-domain forward-speed free-surface Green function (hereinafter referred to as 3DTFFG) approximated by a series obtained by using the principle of stationary phase. King et al. (1988) have shown the added mass and wave-damping coefficients obtained by Fourier transform of the time-domain numerical results. Bingham et al. (1993) have presented the memory functions as well as the impulse response functions of ships using 3DTFFG approximated by Newman (1992). The above mentioned methods are known as the impulse-response function (hereinafter also referred to as IRF) based hydrodynamic formulation which are linear and presented in the moving coordinate system fixed in the mean position of the ship advancing with constant speed of unidirectional velocity.

Lin and Yue (1990) have presented a three-dimensional time domain approach (LAMP) formulated in an earth-fixed coordinate system in order to predict the large-amplitude arbitrary motions and wave loads of a ship in a seaway. In their approach, the body boundary condition is satisfied on the instantaneous wetted surface while the free surface condition is linearized. Their work has further been developed to yield a multi-level code system for linear and nonlinear solutions (Lin et al. 1999).

All the above mentioned methods make use of the free-surface Green function which satisfies the linearized free-surface condition and the constant panel method are employed to obtain numerical solutions. For purely linear problems, using LAMP is more expensive than

using IRF based hydrodynamic formulation since the integral equation is solved at every time-step in the former while the kernel of the integral equation is time invariant in the latter.

In the present paper, the radiation-diff-raction potential boundary value problem is solved by using the Green integral equation associated with 3DTFFG approximated by Newman (1992) under the assumption of Neumann-Kelvin linearization. The integral equations are discretized according to a second-order boundary element method. The Green integral equation at each time-step is solved following the time-stepping procedure presented by Beck and Liapis (1987). The time-domain equation of motion is solved at every time step by using the body-exact Froude-Krylov and restoring forces and moments.

2. FORMULATION

Assuming that the body advances with a constant speed U in the positive x-direction accompanying a small amplitude six-degree-of-freedom motion, the potential can be expressed in a moving coordinate system (x,y,z) attached to the mean position of the body with the origin in the waterplane of the body and the z-axis vertically upwards as follows.

$$\Phi(P,t) = -U\,x + \Phi_W(P) + \sum_{k=1}^{6}\Phi_k(P,t) \qquad (1)$$

where -Ux is the free-stream potential, Φ_W the steady disturbance potential due to the constant forward motion of the body and $\Phi_k\,(k=1,2,,,6)$ the radiation potentials due to the six-degree-of-freedom motion. Adopting the Neumann-Kelvin linearization, the linearized body boundary condition for the unsteady potential, $\Phi_k\,(k=1,2,,,6)$ can be expressed as follows in the moving coordinate system.

$$\frac{\partial\Phi_k}{\partial n} = n_k\dot{x}_k + m_k x_k \quad \text{on } S, k=1,2,...,6 \qquad (2)$$
$$\frac{\partial\Phi_k}{\partial n} = n_k\dot{x}_k + m_k x_k \quad \text{on } S, k=1,2,...,6$$

$$\mathbf{n} = (n_1,n_2,n_3),\ \ \mathbf{r}_O\times\mathbf{n} = (n_4,n_5,n_6) \qquad (3)$$

$$\mathbf{m} = (0,\,0,\,0,\,0,\,Un_3,\,-Un_2) \qquad (4)$$

where, $\mathbf{n}$ and S denote the normal vector and the wetted surface at their mean positions respectively, $\mathbf{r_O}$ the displacement vector with respect to the center of rotation O,, $x_k\,,(k=1,2,,,6)$ the six components of the linear and angular displacement of the body from its mean position and the overdot the time derivative. The initial and boundary conditions for Φ_k are as shown in Liapis and Beck (1985). Representing Φ_k by the following convolution

$$\Phi_k(t) = \int_0^t \phi_k(\tau)\dot{x}_k(t-\tau)d\tau \qquad (5)$$

and applying the body boundary condition due to an impulsive body's velocity

$$\mathbf{n}\cdot\nabla\phi_k(t) = n_k\,\delta(t) + m_k\,H(t) \quad on \ \ S \qquad (6)$$

ϕ_k can be written as follows

$$\phi_k(Q,t) = \varphi_k(Q)\,\delta(t) + \mu_k(Q)\,H(t) + \psi_k(Q,t) \qquad (7)$$

The $\varphi_k(Q)$, $\mu_k(Q)$ and $\psi_k(Q,t)$ can be obtained as solutions of the time-domain Green integral equations (also referred to as Volterra-type integro-differential equation) as shown in Hong and Hong (2008).

The diffraction problem for a body advancing with a constant speed U in transient waves is analogous to the radiation problem. In this case, the total potential is the diffraction

potential Φ_D , the sum of the incident wave potential Φ_0 and the scattering potential Φ_7 .

$$\Phi_D(P,t) = \Phi_0(P,t) + \Phi_7(P,t) \tag{8}$$

In this paper, the diffraction problem is formulated in terms of the time-derivative of the potential $\Phi_{k,t}(P,t) = \partial\Phi_k(P,t)/\partial t$. The body boundary condition is as follows.

$$\frac{\partial\Phi_{7,t}}{\partial n} = -\frac{\partial\Phi_{0,t}}{\partial n} \; on \; S \tag{9}$$

Here, it is assumed that the incident waves in an earth-fixed cartesian coordinate system (x', y', z') take the following form.

$$\varphi_0(x',y',z',t) = \mathrm{Re}\{iA(\omega_0)\frac{g}{\omega_0}\exp[k_0 z' - ik_0(x'\cos\beta + y'\sin\beta) + i\omega_0 t]\}, \; k_0 = \omega_0^2/g \tag{10}$$

where $A(\omega_0)$ denotes the amplitude of this wave train whose absolute frequency is ω_0 and β the angle between the positive x'-axis and the wave propagation direction. When the incident waves are given as an arbitrary impulsive wave elevation, the $\Phi_k(k=0,7)$ can be presented by the following convolution.

$$\Phi_k(t) = \int_{-\infty}^{\infty}\phi_k(t-\tau)\zeta_1(\tau)\,d\tau, \; k = 0,7 \tag{11}$$

where, $\zeta_1(t)$ is the wave elevation at a reference point fixed with respect to the earth-fixed cartesian coordinate system (x', y', z') , $\phi_7(P,t)$ the canonical scattering potential and $\phi_0(P,t)$ the kernel function representing the impulsive incident wave potential when $\zeta(t)$ is given as the delta function $\delta(t)$. The incident wave elevation should be measured at the reference point.

The time-derivative of $\phi_0(P,t)$ has been presented in the moving coordinate system (x,y,z) as follows (Gong 1987).

$$\phi_{0,t}(x,y,z,t) = -\sqrt{\frac{g^3}{4\pi r_0}}\,e^{-\gamma\cos\theta}\,\mathrm{Re}\{e^{i(\theta/2-\gamma\sin\theta)}\,\mathrm{erfc}[i\,sign(t)\sqrt{\gamma}\,e^{i\theta/2}]\} \tag{12}$$

where *erfc( )* denotes the complementary complex error function. It should be noted that Eq.(12) is not applicable in case the waves are incident from abaft the beam of a ship with forward speed. In this case, the initial condition for the present diffraction potential cannot be satisfied and the encounter frequency ω is not a single-valued function of the absolute frequency ω_0.

$$\omega = \omega_0 - Uk_0\cos\beta, \; |\beta| < \pi/2 \tag{13}$$

The diffraction impulse response functions in following seas can be obtained by using the method presented by Korsmeyer and Bingham (1998)

Substituting Eq.(11) into Eq.(9), we have

$$\frac{\partial\phi_{7,t}}{\partial n} = -\frac{\partial\phi_{0,t}}{\partial n} \; on \; S \tag{14}$$

$$\begin{aligned}
&2\pi\phi_{7,t}(P,t) + \iint_S \phi_{7,t}(Q,t)\frac{\partial G^0(P,Q)}{\partial n}dS \\
&+ \int_{-\infty}^{t} d\tau \iint_S \phi_{7,t}(Q,\tau)\frac{\partial G^f(P,Q,t-\tau)}{\partial n}dS \\
&+ \frac{U^2}{g}\int_{-\infty}^{t} d\tau \oint_W d\eta[\phi_{7,t}(Q,\tau)\frac{\partial G^f(P,Q,t-\tau)}{\partial \xi} \\
&- G^f(P,Q,t-\tau)\frac{\partial\phi_{7,t}(Q,\tau)}{\partial\xi}] \\
&- \frac{2U}{g}\int_{-\infty}^{t} d\tau \oint_W d\eta[\phi_{7,t}(Q,\tau)\frac{\partial G_\tau^f(P,Q,t-\tau)}{\partial\xi}] \\
&= -\iint_S \frac{\partial\phi_{0,t}(Q,t)}{\partial n}G^0(P,Q)dS \\
&- \int_{-\infty}^{t}\iint_S \frac{\partial\phi_{0,t}(Q,\tau)}{\partial n}G^f(P,Q,t-\tau)dS
\end{aligned} \tag{15}$$

Applying the Green theorem to $\phi_{7,t}$, the time derivatives of the canonical scattering potential ϕ_7 and the Green function G expressed in the moving coordinate system presented by Newman (1992), the Green integral equation in the time-domain for $\phi_{7,t}$ can be found as follows (Gong 1987).

It should be noted that the kernel of Eq. (15) for $\phi_{7,t}$ is identical to the kernel of the integral equation for the time-domain radiation potentials presented in Liapis and Beck (1985).
The integral equation (15) is discretized spatially by using a second-order boundary element method as shown in Hong and Hong (2008). The numerical integration in time has been carried by using the temporal discretization presented by Beck and Liapis (1987).

3. APPROXIMATE BODY NONLINEAR EQUATIONS OF MOTION and WAVE LOADS

Taking account of the Froude-Krylov and the hydrostatic restoring forces - generalized forces in the sense that they can include moments - calculated over the instantaneous wetted surface of the ship S_t while the forces due to the radiation and scattering potentials on the mean wetted surface S, the following equations of motion of a ship advancing in waves can be obtained as follows.

$$\sum_{k=1}^{6}[(M_{jk}+a_{jk})\ddot{x}_k(t)+b_{jk}\dot{x}_k(t)+c_{jk}x_k(t) + \int_0^t d\tau K_{jk}(t-\tau)\dot{x}_k(\tau) = X_j^7(t)+C_j+g_j+F_j^0(t), j=1,2,...,6 \quad (16)$$

The coefficients M_{jk} denote the ship's inertia matrix and g_j the coefficients due to the gravitational force applied on the mass of the moving body. The coefficients a_{jk} , b_{jk} , c_{jk} and the radiation memory functions K_{jk} are obtained as follows.

$$a_{jk}=\rho\iint_S \varphi_k n_j dS \quad (17)$$

$$b_{jk}=\rho\iint_S (\mu_k - U\frac{\partial \varphi_k}{\partial x})n_j dS \quad (18)$$

$$c_{jk}=-\rho U\iint_S \frac{\partial \mu_k}{\partial x}n_j dS \quad (19)$$

$$K_{jk}(t)=\rho\iint_S [\psi_k(Q,t)-U\frac{\partial \psi_k(Q,t)}{\partial x}]n_j dS \quad (20)$$

As shown above, the hydrodynamic coefficients involving spatial derivatives have been obtained directly without using Stokes'theorem which is valid only for bodies that are wall-sided at the waterline.
The $X_j^7(t),(j=1,2,,6)$ on the right-hand side of Eq.(16), are time-series of the six components of the scattering exciting forces due to a unidirectional incident wave with a heading angle β which can be obtained by convolution as follows

$$X_j^k(t)=\sqrt{1-4U\omega\cos\beta/g} \int_{-\infty}^{\infty} d\tau\, K_j^7(t-\tau)\zeta_I(\tau)\ ,\ j=1,2,,6 \quad for\ k=0\ and\ 7 \quad (21)$$

where ζ_I denotes the wave elevation at the earth-fixed reference point expressed in the moving coordinate system (x,y,z).
$X_j^0(t),(j=1,2,,6)$ for k=o in Eq.(16) denote the six components of the linear Froude-Krylov exciting forces. The Froude-Krylov and

scattering impulse-response functions, $K_j^0(t)$ and $K_j^7(t)$, can be obtained as follows.

$$K_j^k(t) = -\rho \iint_S [\phi_{k,t}(Q,t) - U\frac{\partial \phi_k(Q,t)}{\partial x}] n_j dS, \quad j = 1,2,,,6, \ for\ k = 0\ and\ 7 \tag{22}$$

The linear diffraction impulse-response functions $KD_j(t)$, $(j=1,2,,6)$ are the sum of the Froude-Krylov and scattering impulse-response functions.

The coefficients C_j and $F_j(t)$ denote the approximate body non-linear hydrostatic restoring and Froude-Krylov wave exciting forces respectively. They should be calculated at every time-step over the instantaneous wetted surface under the exact free surface of the incident wave. The incident wave profile may be given by a wave spectrum. In this study, computation of transient response of motions of a body advancing in a regular incident wave has been shown to clarify the present approximate body nonlinear method.

$$\Phi_0(x,y,z,t) = \frac{\zeta_0 g}{\omega_0} e^{k_0 z} \mathrm{Re}\, i e^{i\omega t} \exp\{-ik_0[(x-x_I)\cos\beta + (y-y_I)\sin\beta]\} \tag{23}$$

where, ζ_0 is the wave amplitude at a reference point (x_I, y_I) expressed in the moving coordinate system (x,y,z).

The wave elevation ζ_I at the earth-fixed reference point can be expressed as follows in the moving coordinate system (x,y,z)

$$\zeta_I(x,y,t) = \zeta_0 \cos\{k_0[(x-x_I)\cos\beta + (y-y_I)\sin\beta] - \omega t\} \tag{24}$$

The instantaneous position vector $\mathbf{r}^t_M$ of a point M on the moving body can be expressed as follows.

$$\mathbf{r}_M^t(x,y,z,t) = \mathbf{r}_M^m + \mathbf{D} + \mathbf{\Theta} \times \mathbf{r}_O \tag{25}$$

where $\mathbf{r}^m{}_M$ dnotes the position vector of the point M at its mean position and

$$\mathbf{D} = \sum_{k=1}^{3} x_k \mathbf{e}_k, \quad \mathbf{\Theta} = \sum_{k=4}^{6} x_k \mathbf{e}_{k-3} \tag{26}$$

The instantaneous wetted surface should be determined at every time-step according as the relative height of the point M with respect to the incident wave elevation ζ_I is negative or not.

$$z_M^t(x,y,z,t) = \mathbf{r}_M^t(x,y,z,t) \bullet \mathbf{e}_3 - \zeta_I(x,y,t) \le 0 \tag{27}$$

Then, at every time-step, the approximate body non-linear hydrostatic restoring and Froude-Krylov wave exciting forces can be obtained as follows respectively.

$$C_j(t) = -\rho g \iint_{S_j} dS \mathbf{r}_M^t(x,y,z,t) \bullet \mathbf{e}_3 n_j, \ j = 1,2,...,6 \tag{28}$$

$$F_j(t) = \rho \iint_{S_t} dS\, p_I(x,y,z,t) n_j, \ j = 1,2,,,6 \tag{29}$$

where

$$p_I(x,y,z,t) = \rho g \zeta_0 \exp[k_0 z_M^t(x,y,z,t)] \cos\{k_0[(x_M - x_I)\cos\beta + (y_M - y_I)\sin\beta] - \omega t\} \tag{30}$$

It should be noted that the integration has been done at every time step over S_t , the instantaneous wetted surface of the ship. The equation of motion (16) can be solved by using Newmark-Beta time integrator. The six

components of the wave loads at a station can easily be obtained as follows.

$$W_j^I = X_j^I(t) + C_j^I + g_j^I + F_j^I(t)$$
$$\sum_{k=1}^{6}[(M_{jk}^I + a_{jk}^I)\ddot{x}_k(t) + b_{jk}^I\dot{x}_k(t) + c_{jk}^I x_k(t) \quad (31)$$
$$+ \int_0^t d\tau K_{jk}(t-\tau)\dot{x}_k(\tau) \ , j = 1,2,...,6$$

where the coefficients M_{jk}^l and g_j^l denote respectively the inertia matrix and the gravitational force coefficients of the solid mass bounded by the aft end and the l^{th} station of the ship. The superscript l of the other coefficients indicates that the integration is done over the wetted surface bounded by the aft end and the l^{th} station of the ship

4. NUMERICAL RESULTS AND DISCUSSIONS

Numerical tests for the hydrodynamic forces have been done using the Wigley seakeeping model I (Journée 1992) defined by Eq. (32), advancing in transient head waves at various Froude numbers to show that the present numerical results of the diffraction impulse-response functions compare favorably with the existing experimental and numerical results.

$$2y/B = [1 - 0.8(2x/L)^2 - 0.2(2x/L)^4]$$
$$[1 - (z/D^2)] + (z/D)^2[1 - (z/D)^8]$$
$$[1 - (2x/L)^2]^4, \quad (32)$$
$$L = 6\,meters, \quad L/B = 10, \quad L/D = 16$$

where L, B and D are the length, breadth and draft of the Wigley model respectively.

The mean wetted surface of the Wigley model is discretized as shown in Fig.1. The present time-domain numerical results are referred to as TiMoSBEM (Time-Domain Motion with Second-Order Boundary Element Method). Numerical results of the time-domain forward-speed radiation potential can be found in Hong and Hong (2008) but the hydrodynamic coefficients have been recomputed by using Eqs.(17)-(20) as mentioned earlier.

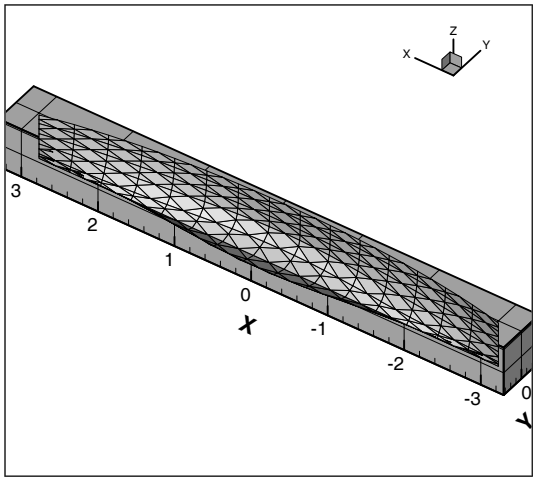

Fig. 1 Second-order panel representation of the Wigley seakeeping model I

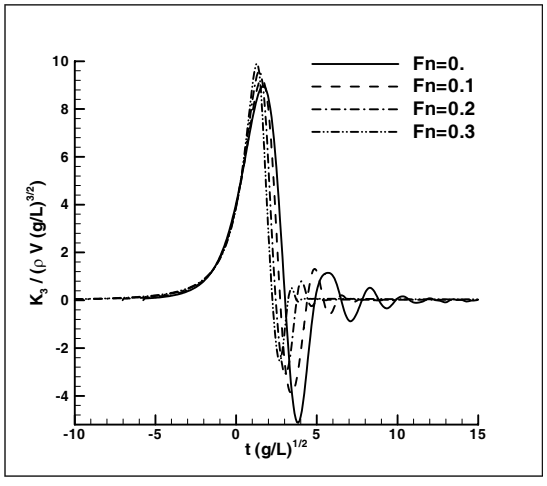

Fig. 2 Heave diffraction impulse response functions of the Wigley model I, β=180 degs.

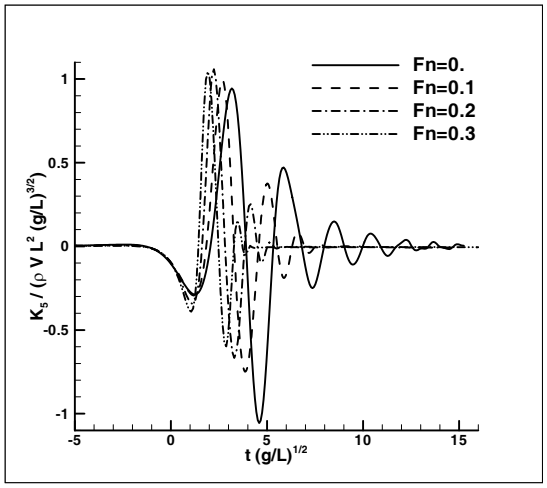

Fig. 3 Pitch diffraction impulse response functions of the Wigley model I, β=180 degs.

Figs.2-3 show heave and pitch diffraction impulse response functions in regular head waves at F_n=0, 0.1, 0.2 and 0.3 obtained by using TiMoSBEM. The Froude number F_n is non-dimensionalized as follows.

$$F_n = U / \sqrt{gL} \tag{33}$$

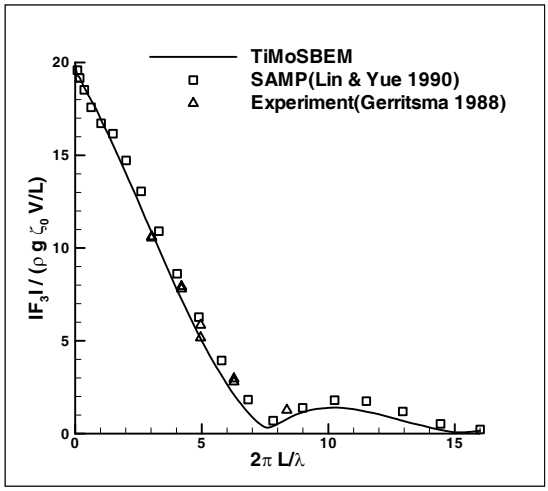

Fig. 4 Heave exciting force coefficients of Wigley model at Fn=0.2, β=180 degs

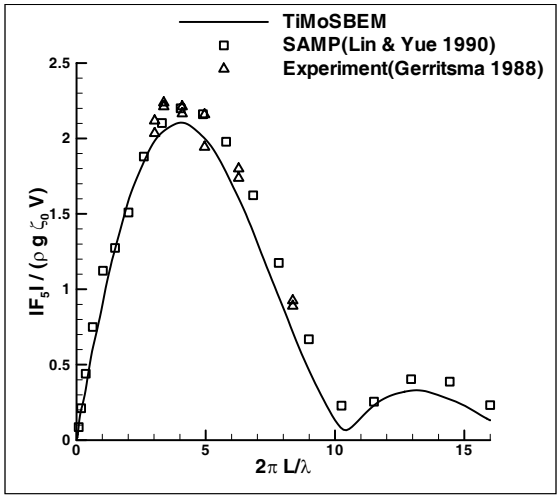

Fig. 5 Pitch exciting moment coefficients of Wigley model at Fn=0.2, β=180 degs

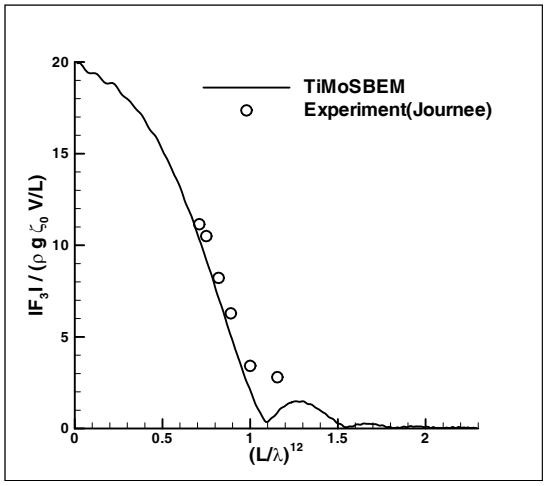

Fig. 6 Heave exciting force coefficients of Wigley model at Fn=0.3, β=180 degs

In Figs.4-5, the frequency-domain heave and pitch exciting force coefficients of the Wigley model at F_n=0.2 calculated from the diffraction impulse response functions via Fourier transform have been compared with the same coefficients obtained from the SAMP forces and moment time histories as presented in Lin and Yue (1990). In Figs.4-5, comparisons with experimental results presented in Gerritsma (1988) have also been made.

In Figs.6-7, the frequency-domain heave and pitch exciting force coefficients of the Wigley model at F_n=0.3 calculated from the diffraction impulse response functions via Fourier transform have been compared with the experimental results presented in Journée (1992).

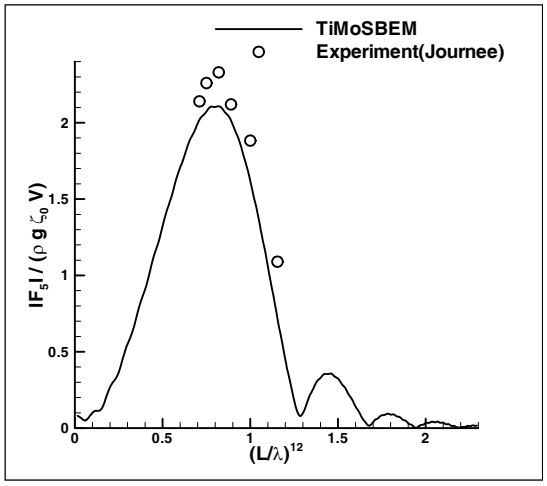

Fig. 7 Pitch exciting moment coefficients of Wigley model at Fn=0.3, β=180 degs

Overall agreement is satisfactory but the present calculations show smaller values. It may be due to numerical errors caused by both the spatio-temporal discretization and truncation of the Fourier integral. Also, it should probably be due to the viscous effects.

A simulation of heave-pitch coupled motion of the Wigley seakeeping model advancing in regular head waves of unit amplitude has been carried out and presented in Hong et al. (2009). Numerical tests for the motions and wave loads have been done using a long rectangular barge model of uniform density having constant sectional area since it is easy to calculate its inertial and buoyancy forces.

The barge advancing at F_n =0.1 in regular head waves has been taken into consideration. The principal particulars of the barge are given in Table 1.

Table 1 Principal particulars of the barge

L	6 m
B	0.6 m
H	0.8 m
draft	0.4 m
z_G	0. m
z_B	-0.2 m
Roll radius of gyration	0.288 m
Pitch radius of gyration	1.74 m
Yaw radius of gyration	1.74m
Displacement	1.44 m^3

The discretized view of the mean wetted surface of the barge is shown in Fig.8. The entire barge is symmetric with respect to the plane z=0. The surface above the mean free surface has also been discretized for the body-nonlinear calculation.

The heave-heave and pitch-pitch memory functions have been shown in Figs.9-10. Figs.11-12 show heave and pitch diffraction impulse response functions of the barge in regular head waves at F_n=0.1. The time histories of the linear heave and pitch Froude-Krylov exciting forces for λ/L=1.15 at F_n=0.1 have been calculated by two different method and presented in Figs.13-14. The curves noted by "Froude-Krylov by convolution" have been obtained by using Eq.(21) and the other by direct integration of the pressure over the mean wetted surface by using Eq.(29). The

agreement between them has been shown to be excellent.

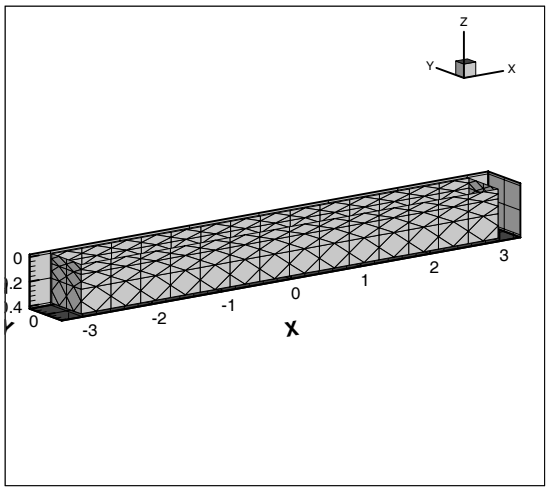

Fig. 8 Second-order panel representation of the mean wetted surface of the barge

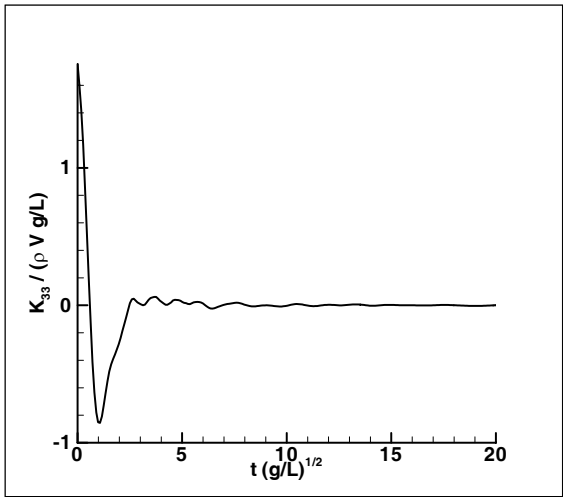

Fig. 9 Heave-heave memory function of the barge at Fn=0.1.

The time histories of the scattering exciting forces have also been presented there. Figs.15-16 show the time histories of the nonlinear heave and pitch responses of the barge for various values of ζ_0 in regular head waves for λ/L=1.15 at F_n=0.1 together with the linear heave and pitch responses. The linear responses have been computed by using the linear restoring forces and the time-series of the diffraction exciting forces obtained by using the convolution of the diffraction impulse-response functions $KD_j(t),(j=1,2,,6)$ following the procedure presented in Hong et al. (1998) and in Hong and Hong (2005).

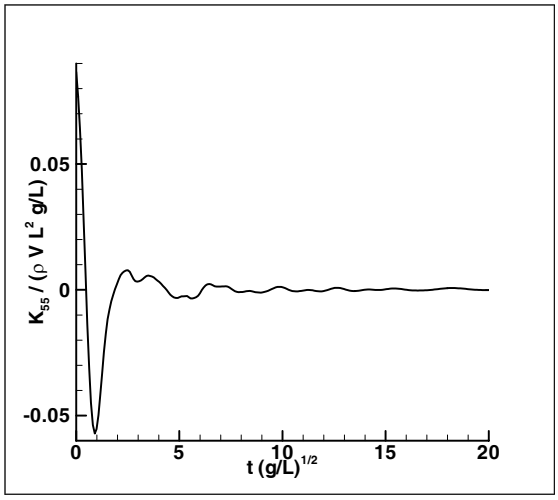

Fig. 10 Pitch-pitch memory function of the barge at Fn=0.1

It has been shown that the linear heave and pitch RAOs of the barge agree very well with the nonlinear RAOs with ζ_0=0.001 meters. It has also been shown that the heave and pitch RAOs of the barge become smaller as ζ_0 increases.

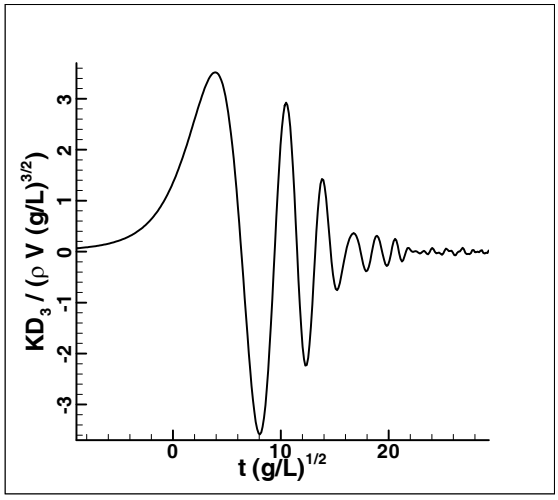

Fig. 11 Heave diffraction impulse response functions of the barge at Fn=0.1, β=180 degs.

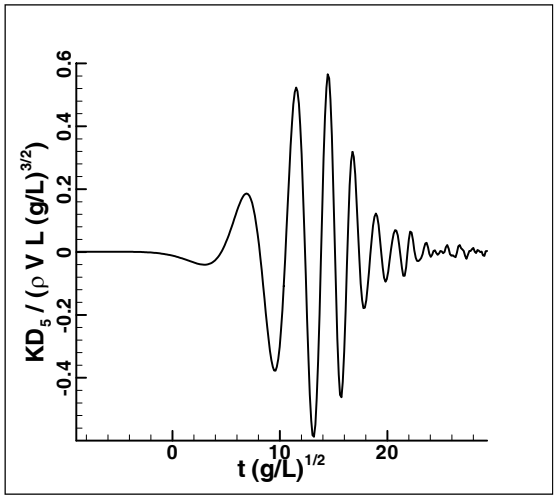

Fig. 12 Pitch diffraction impulse response functions of the barge at Fn=0.1, β=180 degs.

Variations of the nonlinear vertical shear force and bending moment distributions of the barge in regular head waves at Fn=0.1 for λ /L=1.15 with ζ_0=0.2 meters have been shown in Figs.17-18 where n_t denotes the number of time steps.

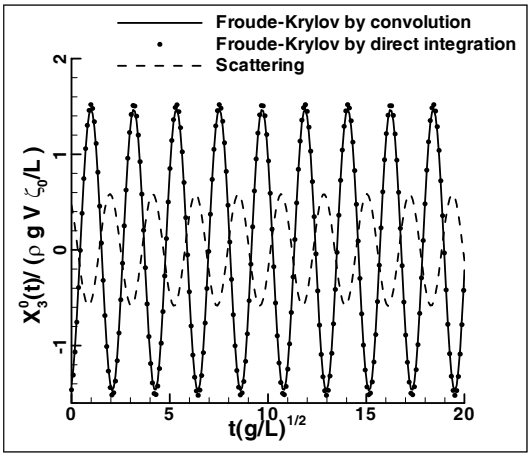

Fig. 13 Time histories of linear Froude-Krylov and scattering heave exciting force of the barge at Fn=0.1, β=180, degs, λ/L=1.15

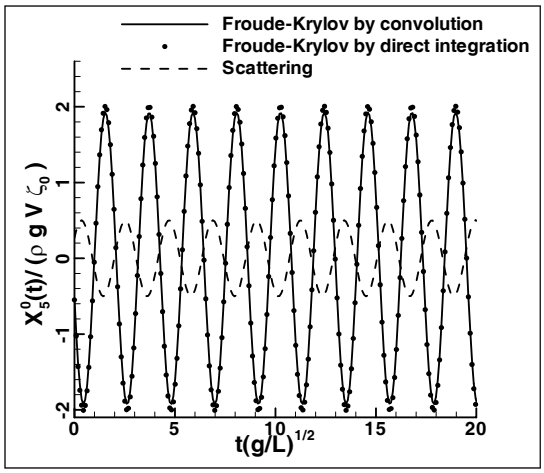

Fig. 14 Time histories of linear Froude-Krylov and scattering pitch exciting moment of the barge at Fn=0.1, β=180, degs, λ/L=1.15

The total number of time steps is 500 for the present numerical tests for the barge.Figs.19-21 show the nonlinear vertical shear force and bending moment distributions of the barge for various values of ζ_0 in regular head waves for λ/L=1.15 at F_n=0.1 together with the linear shear force and bending moment distributions.

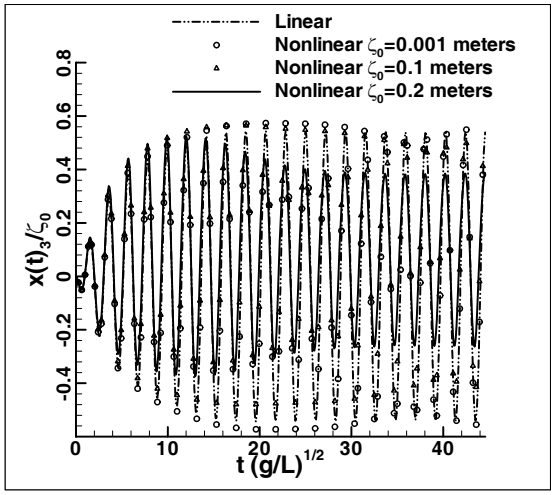

Fig. 15 Time histories of linear and nonlinear heave responses of the barge at Fn=0.1, β=180, degs, λ/L=1.15

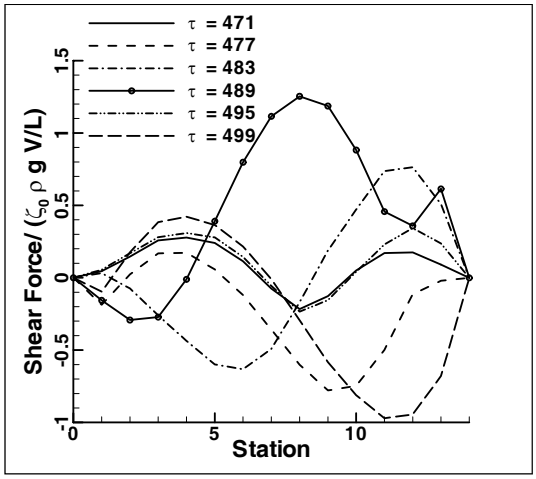

Fig. 17 Variation of the nonlinear vertical shear force distributions of the barge at Fn=0.1, β=180, degs, λ/L=1.15, ζ_0=0.2 m

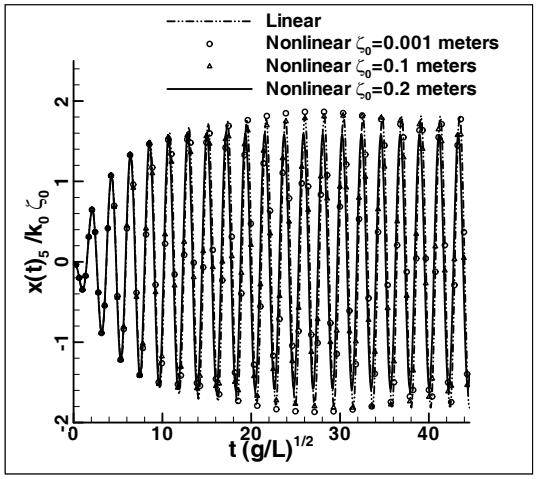

Fig. 16 Time histories of linear and nonlinear pitch responses of the barge at Fn=0.1, β=180, degs, λ/L=1.15

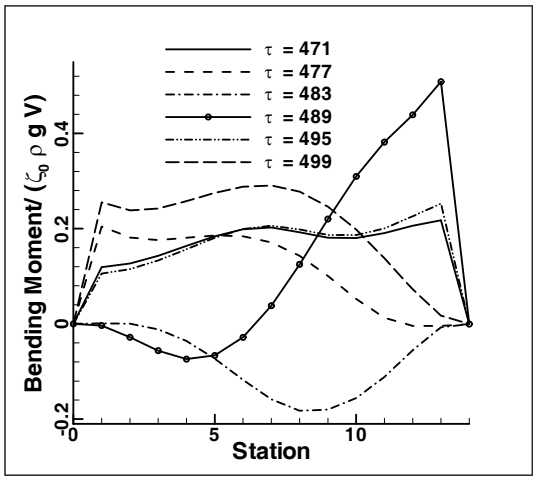

Fig. 18 Variation of the nonlinear vertical bending moment distributions of the barge at Fn=0.1, β=180, degs, λ/L=1.15, ζ_0=0.2 m

In Fig.20, the non-dimensional linear bending moment and the nonlinear bending moment with ζ_0=0.001 meters appear to be 50 times greater than the nonlinear bending moment with $\zeta_0 \geq 0.1$ but the real values of the former are 20 times smaller than the latter.

It has been shown that non-dimensional values of the linear vertical shear force and bending moment distributions of the barge agree very well with the nonlinear values with ζ_0=0.001 meters.

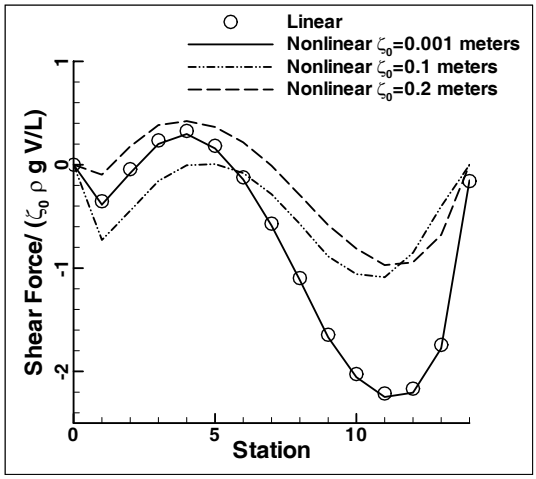

Fig. 19 Linear and nonlinear vertical shear force distributions of the barge at Fn=0.1, β=180, degs, λ/L=1.15

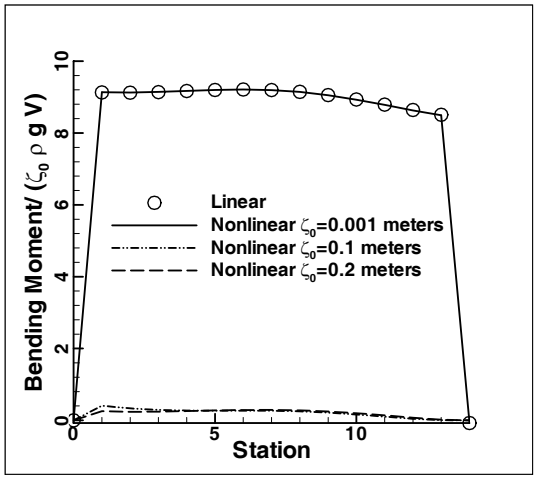

Fig. 20 Linear and nonlinear vertical bending moment distributions of the barge at Fn=0.1, β=180, degs, λ/L=1.15

5. CONCLUSIONS

In this paper, an approximate body nonlinear calculation method for the ship motion and wave loads has been presented. All computations are made on a personal computer.

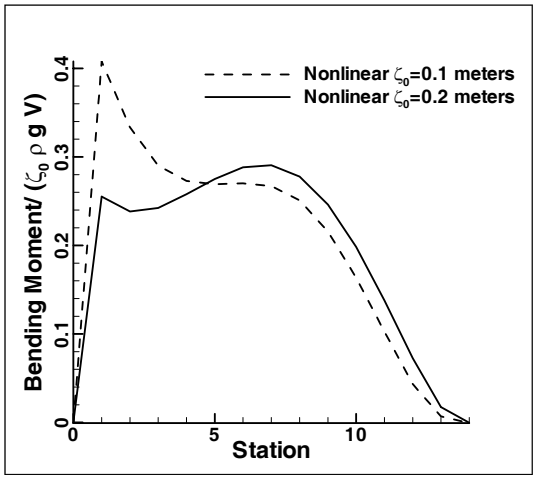

Fig. 21 Enlarged view of nonlinear vertical bending moment distributions of the barge at Fn=0.1, β=180, degs, λ/L=1.15

The diffraction impulse-response functions of the Wigley seakeeping model I advancing in transient head waves at various Froude numbers have been presented. The frequency-domain coefficients of the wave exciting forces and moments obtained via Fourier transform of the diffraction impulse-response functions have been compared with the frequency-domain numerical and experimental results and the agreement between them has been found satisfactory.

The wave exciting forces and moments acting on a ship advancing in plane progressive waves of arbitrary profile can easily be found from convolutions of the incident wave elevation and the diffraction impulse-response functions which may be obtained from the canonical diffraction potential pre-computed once for a Froude number. Comparisons between the linear and the approximate body nonlinear numerical results of motions and wave loads of the barge at a nonzero Froude number have been made. The comparisons show that the present approximate body nonlinear calculation method is consistent.

More numerical results using various hull forms will be presented in the near future. The present method can be used as a practical alternative to predict some significant large amplitude phenomena that the classical linear seakeeping calculation method cannot predict.

Acknowledgments

The present work is a part of the research programs on the development of simulation technology for dynamic stability of ships, supported by the Korea Ministry of Knowledge Economy.

REFERENCES

• Beck, R.F. and Liapis, S.J., 1987. Transient motion of floating bodies at zero forward speed. J. of Ship Research, Vol. 31-3, pp. 164-176.

• Bingham, H.B., Korsmeyer, F.T., Newman, J.N. and Osborne, G.E., 1993, "The Simulations of Ship Motions," Proceedings, 6th Int. Conf. on Numerical Ship Hydrodynamics, pp. 561-579.

• Gerritsma, J. 1988. Motions, wave loads and added resistance in waves of two Wigley hull forms. Rep.No.804, Delft Univ. of Technology, The Netherlands.

• Gong, I. Y. 1987. Time domain analysis of hydrodynamic forces acting on three dimensional bodies (in Korean). Ph.D Thesis, Seoul National University, Republic of Korea.

• Journée, J.M., 1992. Experiments and calculations on 4 Wigley hull forms. Technical report 0909, Ship Hydrodynamics Lab. Delft Univ. of Technology, The Netherlands.

• King, B., Beck, R.F. and Magee, A. 1988. Seakeeping calculations with forward speed using time-domain analysis. Proceedings, 17th Symposium on Naval Hydrodynamics, The Hague, The Netherlands, pp. 577-596.

• Liapis, S. and Beck, R.F. 1985. Seakeeping computations using time-domain analysis. Proceedings, 4th International Conference on Numerical Ship Hydrodynamics. pp. 34-56.

• Lin, W.M. and Yue, D.K.P., 1990. Numerical solutions for large-amplitude ship motions in the time domain. Proceedings 18th Symp. on Naval Hydrodynamics, pp. 41-66.

• Lin, W.M., Zhang, S., Weems, K. and Yue, D.K.P., 1999. A mixed source formulation for nonlinear ship-motion and wave-load simulations. Proceedings 7th Int. Conf. on Num. Ship Hydrodynamics, Nantes, France.

• Hong, S.Y. and Choi, H.S., 1995, "Analysis of Steady and Unsteady Flow around a Ship using a Higher-Order Boundary Element Method (in Korean)," Journal of the Society of Naval Architects of Korea, Vol. 32, No. 1, pp. 42-57.

• Hong, D.C., Jang, L.D., Kim, J.H. and Song, J.Y., 1998, "Computation of 3-D Vertical Shear Force and Bending Moment on a Ship Floating in Regular Waves bodies (in Korean)," Proceedings, Annual Spring Meeting of the Society of Naval Architecture of Korea, pp. 276-279.

• Hong, D.C. and Hong, S.Y., 2005, "Waveload Analysis for Heeled Barges with Flooded Compartiments (in Korean)," Journal of the Society of Naval Architects of Korea, Vol. 42, No. 4, pp. 379-387.

• Hong, D.C. and Hong, S.Y., 2008. “Numerical study of the radiation potential of a ship using the 3D time-domain forward-speed free-surface Green function and a second-order BEM,”Journal of the Society of Naval Architects of Korea Vol. 45, No. 3, pp.258-268.

• Hong, D.C., Sung, H.G. and Hong, S.Y., 2009, “Numerical Tests of Large Amplitude Ship Motion with Forward Speed in Severe Seas,” OMAE 2009-79277, Proceedings ASME 28th International Conference on OMAE, Honolulu, Hawaii, USA.

• Newman, J.N., 1992. Approximation of free-surface Green functions. Wave Asymptotics, Proceedings Fritz Ursell Meeting, Cambridge Univ. Press, pp. 107-135.

• Stoker, J.J., 1957. Water waves. Inter-sciencePublishers, New York, pp. 187-196.

< 홍 도 천 >

< 홍 사 영 >

< 성 홍 근 >